Protein Trapping

Trapping of Proteins under Physiological Conditions in a Nanopipette**

Richard W. Clarke, Samuel S. White, Dejian Zhou, Liming Ying, and David Klenerman**

Dielectrophoresis (DEP) uses the directed motion of particles caused by polarization effects in a nonuniform electric field,[1] and it has proved to be a powerful tool in performing sample sorting,[2–6] trapping,[6–8] and manipulation[6,9–11] on micrometer- and submicrometer-sized particles to date. These experiments have been largely performed in low-conductance solutions by using metal electrodes—conditions that are nonphysiological and in which damage by electrolysis is also possible. Herein, we use a nanopipette for electrodeless dielectrophoresis and show clear evidence, by using wide-field fluorescence imaging, for the reversible trapping of Alexa-488-labeled proteins (protein G and immunoglobulin G (IgG)) and also of the fluorophore alone. Our results show a dielectrophoretic concentration enhancement for these fluorophore-labeled proteins of at least a factor of 300. This concentration enhancement was shown to take place in less than a second and to be within about a factor of two of that observed with DNA. This finding opens up new possibilities for miniaturized bioanalysis.

Previous applications of DEP have focused on the separation of micrometer- and submicrometer-scale objects, such as cells,[9] viruses,[10] and colloidal particles,[12] and the manipulation and trapping of long DNA molecules.[7] More recently, DEP has been applied as a bottom-up approach to assemble functional structures by using nanosized building blocks[13–16] and submicrometer-diameter fibrils from single-wall carbon nanotubes.[17] DEP has also been utilized in separating metallic carbon nanotubes from semiconducting carbon nanotubes,[18] and evidence for the trapping of bovine serum albumin has been presented.[19] All of these studies have used metallic microelectrodes for their DEP traps. These have the advantage of flexible designs for the electrodes and a relatively low voltage being required to generate a high-field gradient on the microscale. However, there are limitations in the application of trapping by metallic DEP. Firstly, it is not compatible with biological samples, as the low-ionic-strength solutions that are used will lead to unfolding of DNA and proteins. Secondly, proteins will be easily drawn to the metal surface of the electrodes where they will become denatured. Thirdly, complex electrochemical reactions such as electrolysis may occur at the microelectrodes. These reactions not only generate gas bubbles that interfere with trapping but they may also damage the trapped molecules and degrade the electrodes. This is a particular problem at the predicted high electric fields required to trap proteins.[20] To address this problem, Chou and co-workers developed DEP traps by patterning geometrical constrictions in an insulating quartz substrate instead of the traditional metallic microelectrodes.[21] The constrictions in a microfluidic channel are used to create a high-field gradient with a local maximum; DNA was successfully trapped in this high-field region under ionic buffer conditions. Recently, we used a laser-pulled glass nanopipette filled with ionic buffer to generate a high-field gradient near the pipette tip.[22] We have shown that DNA and proteins maintain their functionality after passing through this high electric field in the pipette tip.[23] We have also probed the motion of fluorophore-labeled double- and single-stranded 40-mer DNA, a one kilobase single-stranded DNA, and a single nucleotide triphosphate (deoxycytidine 5′-triphosphate, dCTP) just inside and outside the pipette tip at different frequencies and amplitudes of applied voltages.[22] A strong trapping effect was observed during the negative half cycle for all DNA samples and also for dCTP. DNA might have been a special case for the trapping of molecules by DEP since it is a highly charged polyelectrolyte because of its phosphate backbone. Herein, we present unequivocal evidence of the reversible trapping of proteins in the nonuniform electric field generated in the tip of a nanopipette, by using fluorescence microscopy with wide-field illumination.

A schematic representation of the experimental setup is shown in Figure 1. The borosilicate glass pipettes have a 3–6° half-cone angle and an inner diameter of 100–150 nm. The pipette and bath solution contain 100–150 mM sodium chlo-

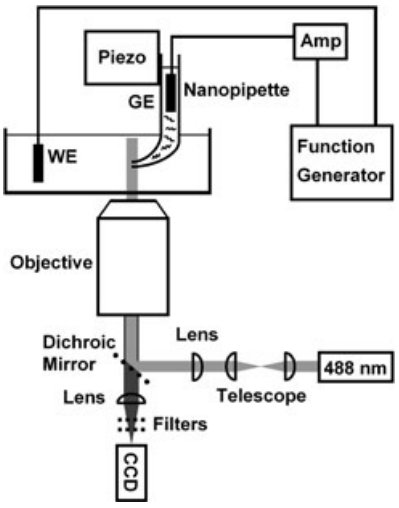

Figure 1. Schematic of the experimental setup used. Amp = current and voltage amplifier ($\times 10^8$), Piezo = piezoelectric nanopositioning stage, WE = working electrode, GE = ground electrode, CCD = charge-coupled device.

[*] R. W. Clarke,[+] S. S. White,[+] Dr. D. Zhou, Dr. L. Ying, Dr. D. Klenerman
Department of Chemistry
University of Cambridge
Lensfield Road, Cambridge (UK)
Fax: (+44) 1223-336-362
E-mail: ly206@cam.ac.uk
dk10012@cam.ac.uk

[+] These authors contributed equally to this work.

[**] This work was funded by the Biotechnology and Biological Sciences Research Council (BBSRC), UK. We thank Universal Imaging Corporation, UK, for the loan of the Photometrics CCD camera and MetaMorph software.

Supporting Information for this article is available on the WWW under http://www.angewandte.org or from the author.

 DOI: 10.1002/ange.200500196

ride. An electric field is generated in the tip of the pipette on application of a voltage between the electrodes in the pipette (GE) and bath (WE). In these experiments, the pipette electrode was earthed and a voltage was applied to the bath electrode. Application of 1 V results in a maximum electric field of about $10^6\ V\,m^{-1}$ in the pipette tip.[22] We used wide-field illumination of the pipette by using an expanded 488-nm laser beam and detected the fluorescence with a CCD camera. This enabled the spatial distribution of fluorophore-labeled biomolecules in the pipette on application of different voltages to be examined.

We studied protein G and IgG labeled with multiple Alexa-488 fluorophores, and as a comparison we also studied a single-stranded 20-mer DNA labeled with a Rhodamine Green fluorophore. When certain potential differences were applied between the two electrodes, we observed fluorescence in an area close to the tip; this fluorescence is proportional to the concentration of molecules, a fact allowing us to confirm that the molecules must be trapped in this tip region. Qualitatively, all these samples showed the same trapping behavior: Figure 2 A–D shows representative wide-field images obtained at −5, −1, +1, and +5 V, respectively, with protein G in the pipette. There is weak localization at +1 V, but a clear, confined build-up of protein G occurs upon application of −5 V. Once the electric field is removed, the trapped protein molecules quickly disperse away by simple diffusion in less than a second. Figure 2 E shows a line scan along the nanopipette at −5 V: protein G is clearly localized very close to the pipette tip in a region with a full width at half maximum of (990 ± 80) nm. The observed trap is also completely reversible: when a sine wave is applied (0.5 Hz) at either 1 or 5 V, cycles of "trapping" followed by "release" are seen. Videos of this time-dependent behavior of the pipette upon application of a sine wave at 0.1 Hz with an amplitude of 1 V (Movie 1) and 5 V (Movie 2) are shown in the Supporting Information.

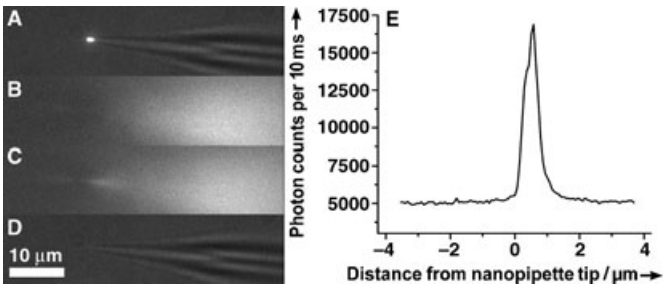

Figure 2. A)–D) Representative wide-field fluorescence images showing the dependence of protein G concentration in the nanopipette on applied voltage: A) −5, B) −1, C) +1, D) +5 V. The nanopipette was wide-field illuminated by a 7-mW laser beam at 488 nm and contained 100 nM Alexa-488-labeled protein G in PBS buffer, the same buffer solution as in the bath. Images (A) and (D) were recorded with very low background illumination to simultaneously record the pipette position and fluorescence (exposure time 10 ms). Images (B) and (C) were recorded without background illumination (exposure time 100 ms). E) Line scan along the axis of a wide-field illuminated nanopipette filled with the same solution as used for (A)–(D) and with the bath electrode at −5 V.

A representative graph of the dependence of the fluorescence intensity of the trapped protein G with applied voltage is shown in Figure 3. It is clear from the Figure that the protein G concentrates at the tip of the pipette below a voltage of −5 V. There is also a far smaller population build-up at approximately +2 V. Comparison of the fluorescence intensity at zero-applied voltage with the highest integrated fluorescence intensity allows us to estimate the concentration enhancement in the pipette tip. This value varied between pipettes, because of variation in size and taper angle, but was always in the range of 300–3000. IgG gave similar concentration enhancements.

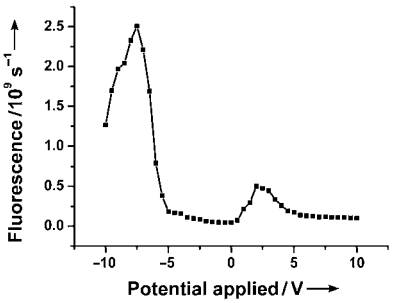

Figure 3. Integrated fluorescence response of the protein G solution in a nanopipette to applied voltage. The nanopipette tip was wide-field illuminated at 488 nm and contained 100 nM Alexa-488-labeled protein G. The intensity of the fluorescence was integrated in the same small trap region. All experiments were performed in PBS buffer, the same buffer solution as in the bath. Fluorescence data were derived from images of 1-ms time resolution and were acquired 2 s after the bath electrode changed polarity to the value indicated.

We compared the enhancement in protein G concentration with that for single-stranded 20-mer DNA in the pipette under the same experimental conditions. The DNA gave a concentration enhancement approximately two times larger than protein G (600–6000) and also showed the onset of trapping at about half the applied voltage. A video of the DNA trapping in the pipette is shown in the Supporting Information (Movie 3). Similar concentration enhancements were observed when using a DC voltage rather than an AC voltage. The number of trapped molecules did not increase significantly with time, since there is a very low rate of flow of molecules to the tip once a negative voltage has been applied to the bath electrode. To test whether the trapping was dye dependant, Alexa-647-labeled IgG was investigated. Exactly the same trapping phenomenon as with Alexa-488-labeled IgG and protein G was observed, a result indicating that the trapping of the protein is not dye specific.

We also studied the free Alexa-488 dye to determine how much the dye contributed to the observed trapping. The onset of strong trapping occurred at approximately −1.1 V—a lower amplitude of voltage than that observed with the DNA and the proteins. Another key difference is that the trap was much larger than that with either the proteins or the DNA, as shown in Figure 4. The dye trap is approximately 8 μm in length. These observations indicate that not only the dye but also the protein or DNA has an effect on the trapping voltage and the size of the trap region.

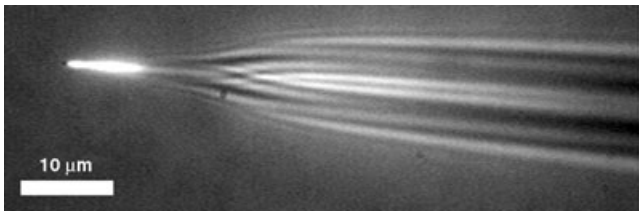

Figure 4. Fluorescence image recorded by using wide-field illumination (5.2 mW) of a nanopipette filled with 100 nM Alexa-488 dye in PBS buffer, the same buffer solution as in the bath. At −2 V there is a large dielectrophoretic concentration of dye confined to the first 8 μm of the nanopipette tip. This image was acquired with an exposure time of 1 s.

The net electric-field-induced force acting on the biomolecules in the nanopipette is a result of the combination of three components: electroosmosis, electrophoresis, and dielectrophoresis. The direction and magnitude of these forces depend on the applied voltage and the position of the molecules in the pipette. In particular, the dielectrophoretic force is proportional to the square of the electric field and will be largest at the pipette tip.[22] Here, we have applied higher voltages (up to 10 V) than we have used previously for controlled delivery (up to 400 mV) to increase the magnitude of the dielectrophoretic effect. Protein G is negatively charged under the conditions of this experiment and the contribution of electroosmotic flow is small,[22] so at a positive applied voltage the electrophoretic force and dielectrophoretic force act in the same direction to pull protein G out of the pipette tip. It appears that there is a range of voltages (1.5–3.5 V) at which some build-up of protein occurs in the tip but the protein is still able to flow out of the pipette. By contrast, on the application of a negative voltage the dielectrophoretic force opposes the electrophoretic force. Hence, close to the tip the two forces balance, and trapping can occur in a small, localized region inside the tip without any flow either to the bath solution or to the capillary electrode.

This work has demonstrated that, under the same experimental conditions, proteins can be trapped with an increase in concentration that is within a factor of two of that observed with DNA. There seems to be no theoretical basis for this observation and it was not expected. While there is clearly a contribution from the dye, there also appears to be a significant contribution from the protein as well. The observed trapping by DEP at DC or low-frequency AC voltages may reflect the contribution of the structured water molecules and counterions around the biological molecule to the dipole induced under these high electric fields, rather than the structure of the biomolecule itself. This will need further experimental and theoretical investigation.

In summary, we have shown that we can trap nanometer-sized proteins, as well as DNA, in physiological buffer. This results in concentration enhancements of at least a factor of 300, with this enhancement obtained in less than a second. Extension of this methodology to the single-molecule limit should be possible with optimization of the trap geometry, thereby allowing prolonged solution studies of individual molecules. Practically, this is a new and potentially powerful method to trap, concentrate, and manipulate both DNA and proteins. It could be used as the basis of ultrasensitive and highly miniaturized bioassays, particularly when performed in parallel in two-dimensional nanofabricated devices.

Experimental Section

The protocol in the Alexa Fluor 488 (Alexa-488) protein-labeling kit provided by Molecular Probes (USA) was employed to label rabbit IgG. Briefly, 1M freshly prepared sodium bicarbonate solution (50 μL) was added to rabbit IgG (0.5 mL, 2 mg mL^{-1}) in phosphate-buffered saline (PBS) buffer to adjust the pH value of the solution to about 8.3. The combined solution was then transferred to a vial of Alexa-488 reactive dye, and the mixture was gently stirred for 1 h at room temperature. The reaction mixture was then loaded on a purification resin column supplied with the kit, to separate the protein from the unreacted dye, and washed once with eluting buffer to give a purity of $>99\,\%$. The labeled rabbit IgG was in the first fluorescent band. The degree of labeling was determined by measuring the UV absorbance at 280 and 494 nm, by using the equations provided by Molecular Probes (USA). The average labeling was 7 Alexa-488 fluorophores per IgG molecule. HPLC-purified 20-base oligonucleotide 5′-CTATGCAGCCATTGTAGTCC-3′ (IBA, Germany) was labeled at the 3′ terminus with the fluorophore Rhodamine Green. Protein G was purchased from Molecular Probes (USA). The average labeling was 2.3 Alexa-488 fluorophores per protein G molecule.

The nanopipettes, with inner radii of around 50 nm, were made by using a laser-based pipette puller (Model P-2000, Sutter Instrument Co., USA), and a two-line program was used to pull borosilicate glass capillaries (inner diameter = 0.58, outer diameter = 1 mm), with the following parameters: Heat = 350, Fil = 3, Vel = 30, Del = 220, Pull and Heat = 330, Fil = 2, Vel = 27, Del = 180, Pull = 250.

For the pipette experiments, a 100 nM DNA, 100 nM protein, or 100 nM Alexa-488 dye solution was backfilled to the bent nanopipette by a microfiller (Microfil 34, World Precision Instruments, USA). A coverglass-bottomed dish (Willco Wells GWST-1000, Netherlands) containing buffer (2–3 mL) was used as the bath. A home-built nanomanipulation system consisting of a piezoelectric translational stage (Tritor 38, Piezosystem Jena, Germany) was used to position the nanopipette. The pipette tip was placed 5–10 μm above the dish surface. A voltage was applied to the nanopipette through two Ag/AgCl electrodes, one in the bath and the other inside the pipette, which served as the working and ground electrodes, respectively. The ion-current flow through the pipette was amplified by a high-impedance amplifier and monitored by an oscilloscope. The ion current flowing through the pipette was the same in the presence and absence of DNA or protein since the ion current is dominated by the flow of sodium and chloride ions. In addition, no ion-current reduction because of partial blocking could be detected with DNA, protein, or antibody in the pipette. Identical buffers were used both in the pipette and in the bath. For the DNA experiments, buffer (10 mM tris(hydroxymethyl)aminomethane hydrochloride (Tris-HCl), 1 mM ethylenediaminetetraacetate (EDTA), and 100 mM NaCl at pH 7.4) was used with EDTA added to remove multivalent cations in the solution. For the protein and dye experiments, a different buffer (10 mM phosphate, 150 mM NaCl, 2 mM NaN_3 at pH 7.2) was used.

A home-built wide-field fluorescence microscope was used to record images of the trapping of dye-labeled biomolecules in the nanopipette. Laser beams (488 nm, Argon ion, model 35LAP321–230, Melles Griot, USA) were spatially filtered and collimated before being sent to the microscope. A home-built fluorescence microscopy attachment was mounted to the rear port of a TE2000U optical microscope (Nikon, USA). The laser beam was focused to the back focal point of an oil immersion objective (Apochromat 60×, NA 1.45, Nikon, USA) after passing through a dichroic mirror (FITC/CY5, AHF Analysentechnik AG, Germany). Fluorescence was collected by

the same objective, filtered by a bandpass filter (535 AF45, Omega Optical, USA) and imaged onto a CCD camera (see Figure 1). The potential waveforms applied to the electrodes were created by using a function generator (Model DS345, Stanford Research Systems, USA).

All experimental data (except for Figure 4) were acquired by using a Photometrics Cascade 512B High Speed CCD camera (Roper Scientific, USA) and a PICOLO Pro 2 video capture card (Euresys Inc., USA). The data for Figure 4 were acquired by using a Watec WAT-902H CCD camera (Watec, Japan). The conversion of the raw video format into AVI format was performed by using the VirtualDub 1.4.10 program (Build 13870).

Received: January 18, 2005
Published online: May 10, 2005

Keywords: biomolecule trapping · DNA · electrophoresis · nanotechnology · proteins

[1] H. A. Pohl, *Dielectrophoresis*, Cambridge University Press, Cambridge, **1978**.
[2] M. Washizu, S. Suzuki, O. Kurosawa, T. Nishizaka, T. Shinohara, *IEEE Trans. Ind. Appl.* **1994**, *30*, 835.
[3] B. H. Lapizco-Encinas, B. A. Simmons, E. B. Cummings, Y. Fintschenko, *Anal. Chem.* **2004**, *76*, 1571.
[4] H. Morgan, M. P. Hughes, N. G. Green, *Biophys. J.* **1999**, *77*, 516.
[5] N. G. Green, H. Morgan, *J. Phys. D* **1997**, *30*, L41.
[6] M. P. Hughes, *Nanotechnology* **2000**, *11*, 124.
[7] C. L. Asbury, A. H. Diercks, G. van den Engh, *Electrophoresis* **2002**, *23*, 2658.
[8] C. L. Asbury, G. van den Engh, *Biophys. J.* **1998**, *74*, 1024.
[9] T. Schnelle, T. Müller, R. Hagedorn, A. Voigt, G. Fuhr, *Biochim. Biophys. Acta* **1999**, *1428*, 99.
[10] M. P. Hughes, H. Morgan, F. J. Rixon, J. P. H. Burt, R. Pethig, *Biochim. Biophys. Acta* **1998**, *1425*, 119.
[11] Y. Huang, K. L. Ewalt, M. Tirado, T. R. Haigis, A. Forster, D. Ackley, M. J. Heller, J. P. O'Connell, M. Krihak, *Anal. Chem.* **2001**, *73*, 1549.
[12] R. Pethig, Y. Huang, X. B. Wang, J. P. H. Burt, *J. Phys. D* **1992**, *25*, 881.
[13] R. Krupke, F. Hennrich, H. B. Weber, M. M. Kappes, H. von Lohneysen, *Nano Lett.* **2003**, *3*, 1019.
[14] X. Q. Chen, T. Saito, H. Yamada, K. Matsushige, *Appl. Phys. Lett.* **2001**, *78*, 3714.
[15] K. D. Hermanson, S. O. Lumsdon, J. P. Williams, E. W. Kaler, O. D. Velev, *Science* **2001**, *294*, 1082.
[16] X. F. Duan, Y. Huang, Y. Cui, J. F. Wang, C. M. Lieber, *Nature* **2001**, *409*, 66.
[17] J. Tang, B. Gao, H. Z. Geng, O. D. Velev, L. C. Qin, O. Zhou, *Adv. Mater.* **2003**, *15*, 1352.
[18] R. Krupke, F. Hennrich, H. von Lohneysen, M. M. Kappes, *Science* **2003**, *301*, 344.
[19] L. Zheng, J. P. Brody, P. J. Burke, *Biosens. Bioelectron.* **2004**, *20*, 606.
[20] L. Zheng, S. Li, P. J. Burke, J. P. Brody, *Proc. Third IEEE Conf. Nanotech.* **2003**, p. 437.
[21] C. F. Chou, J. O. Tegenfeldt, O. Bakajin, S. S. Chan, E. C. Cox, N. Darnton, T. Duke, R. H. Austin, *Biophys. J.* **2002**, *83*, 2170.
[22] L. M. Ying, S. S. White, A. Bruckbauer, L. Meadows, Y. E. Korchev, D. Klenerman, *Biophys. J.* **2004**, *86*, 1018.
[23] A. Bruckbauer, D. J. Zhou, L. M. Ying, Y. E. Korchev, C. Abell, D. Klenerman, *J. Am. Chem. Soc.* **2003**, *125*, 9834.

